ITG Turbulence

Lecture by Professor P.H. Diamond,
notes by A.R. Knyazev

1 Introduction

The ion-temperature-gradient (ITG), a.k.a. the η_i mode,

$$\eta_i = \frac{d\ln T_i}{d\ln n}, \tag{1}$$

is another basic paradigm from the theory of transport in tokamaks. It is an important example of reactive instability, i.e. instability that does not require dissipation. This lecture presents the phenomenology related to ITG, illustrates the negative compressibiliry nature of the ITG instability with the simplest physical model, and discusses the implications of ITG for the energy transport and for the inward pinch of density.

Importance of ITG in the tokamak energy transport was definitively demonstrated in the pellet-injection experiments performed on the ALCATOR as shown in Fig 1. Without • the pellet injection, the energy confinement scaling obtained from experiments demonstrates the transition from linear $\tau_E \propto n$ to saturated Ohmic confinement (the **LOC** $\rightarrow$ **SOC** transition), occurring due to the collisional coupling between Ohmically heated electrons and the ions. Experiments with ∘ pellet injection removed the τ_E saturation, by steepening the density gradient ∇n and thus decreasing η_i.

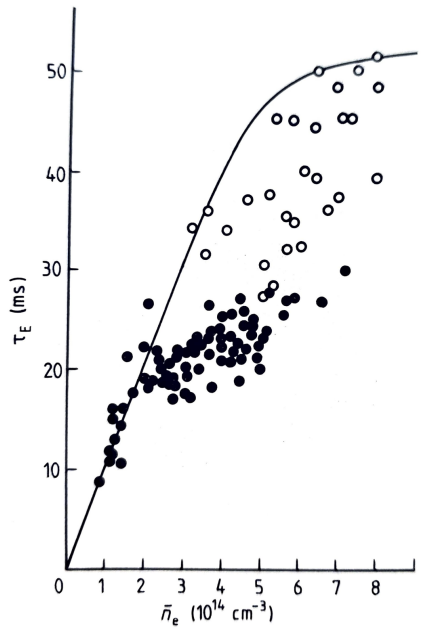

Figure 1: The energy confinement time τ_E vs density $\bar{n}_e$ in ALCATOR experiments, with ∘ and without • the pellet injection

Although the pellet injections were motivated by the difficulty of edge fueling and were not intended to improve confinement, observed recovery of the LOC scaling demonstrated that peaked density profiles are good for energy confinement. This was direct evidence for anomalous transport in agreement with the η_i-mode analysis, and so the importance of ITG for energy transport in tokamaks was recognized.

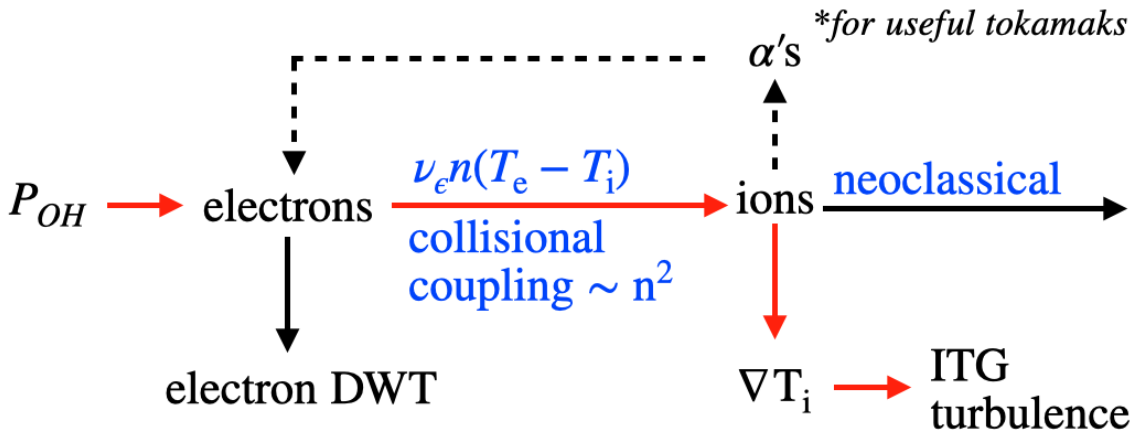

The thermal diffusivity goes as $\chi \sim 1/n$ in LOC. Suppressing the η_i mode by pellet injection leaves electron drift waves as the only energy sink. The heat pulse propagation experiments done in the pellet states resulted in $\tau_{HPP} \sim n$, and hence implicitly $\chi \sim 1/n$, which also supports the recovery of LOC by peaking the density profile.

2 Simple ITG example

2.1 Derivation

To illustrate the onset of ITG instability, employ a fluid model for plasma with density and temperature gradients $T_i(x, y)$, $n(x, y)$, located in the uniform magnetic field $B\mathbf{e}_z$. The continuity equation is

$$\frac{\partial n}{\partial t} + \nabla \cdot (n\mathbf{v}) = \frac{\partial n}{\partial t} + (\nabla n) \cdot \mathbf{v}_\perp + n(\nabla_\perp \mathbf{v}_\perp + \nabla_{||} v_{||}) = 0, \tag{2}$$

where

$$\mathbf{v}_\perp = \frac{\mathbf{E} \times \mathbf{B}}{B^2} = -\frac{\nabla\tilde{\Phi} \times \mathbf{B}}{B^2} = -\frac{\nabla \times (\tilde{\Phi}\mathbf{B})}{B^2}. \tag{3}$$

Linearized for perturbations $\tilde{n}$, $\tilde{v} \sim \exp(ik_y y + k_z z - \omega t)$, $\mathbf{v}_\perp = -ik_y\tilde{\Phi}\mathbf{e}_{\mathrm{x/B}}$ and Eq. (2) becomes

$$-\omega\frac{\tilde{n}}{n} - \frac{d\ln(n)}{dx}\frac{\tilde{k}_y}{B}\tilde{\Phi} + k_z\tilde{v}_{||} = 0. \tag{4}$$

The parallel velocity component $\tilde{v}_{||}$ is given by force balance along $\mathbf{B}$,

$$m_i n(\frac{\partial \mathbf{v}_{||}}{\partial t} + \mathbf{v}_\perp \cdot \nabla v_{||}) = -\nabla_{||}\tilde{p}_i - n|e|\nabla_{||}\tilde{\Phi}. \tag{5}$$

After linearization, Eq. (5) becomes

$$\omega m_i n\tilde{v}_{||} = k_z(\tilde{p} + |e|n\tilde{\Phi}). \tag{6}$$

Assuming adiabatic response from electrons, the ion temperature T_i can be obtained from the ion's equation of state $pV^{5/3} = const$, which implies

$$\frac{d(pn^{-5/3})}{dt} = \frac{\partial(pn^{-5/3})}{\partial t} + \mathbf{v} \cdot \nabla(\frac{p}{n^{5/3}}) = 0, \tag{7}$$

or, after linearization,

$$\frac{\tilde{p}}{p} - \frac{5}{3}\frac{\tilde{n}}{n} + \frac{ik_y}{\omega B}\tilde{\Phi}(\frac{d\ln p}{dx} - \frac{5}{3}\frac{d\ln n}{dx}) = 0. \tag{8}$$

Recalling that from $pV^{5/3} = const$ follows

$$\frac{dp}{p} - \frac{5}{3}\frac{dn}{n} = \frac{dT}{T} - \frac{2}{3}\frac{dn}{n} = 0, \tag{9}$$

force balance (8) can be rewritten as

$$\frac{\tilde{p}}{p} - \frac{5}{3}\frac{\tilde{n}}{n} + \frac{ik_y}{\omega B}\tilde{\Phi}\frac{d\ln n}{dx}(\eta_i - \frac{2}{3}) = 0. \tag{10}$$

The perturbation density of ions then can then be expressed from (4, 6 ,11) as

$$\frac{\tilde{n}}{n} + \frac{k_y\tilde{\Phi}}{\omega B}\frac{d\ln n}{dx} = \left(\frac{k_z}{\omega}\right)^2\frac{T_i}{m_i}\left[\frac{5}{3}\frac{\tilde{n}}{n} + \frac{k_y}{B\omega}(\eta_i - \frac{2}{3})\frac{d\ln n}{dx}\tilde{\Phi} + \frac{|e|\tilde{\Phi}}{T_i}\right] \tag{11}$$

Equating the ion density to the adiabatic response from the electrons $|e|\tilde{\Phi}/T_e$ for perturbations with the spatial scale greater than the Debye radius gives dispersion relation

$$1 - \frac{\omega_{*e}}{\omega} - \left(\frac{k_z}{\omega}\right)^2\frac{T_i}{m_i}\left[\frac{5}{3} + \frac{T_e}{T_i} + \frac{\omega_{*e}}{\omega}\left(\eta_i - \frac{2}{3}\right)\right] = 0, \tag{12}$$

where

$$\omega_{*e} = -\frac{k_y T_e}{eB}\frac{d\ln n}{dx} = 0. \tag{13}$$

Dispersion relation (12) implies that high frequency $\omega \gg \omega_{*e}$ perturbations result in sound waves, while the low frequency $\omega \ll \omega_{*e}$ can result in instability for $\eta_i > 2/3$,

$\omega \gg \omega_{*e}$	$\omega \ll \omega_{*e}$
$\omega^2 = \frac{k_z^2}{m_i}(T_e + \frac{5}{3}T_i) > 0$ (14)	$\omega^2 = \frac{k_z^2 T_i}{m_i}(\frac{2}{3} - \eta_i)$, can have $\omega^2 < 0$ (15)

The value 2/3 for stability threshold comes from the equation of state (9) for ions, i.e. $C_p/C_v - 1$ which is 2/3 for mono-atomic gas. It is important to note however that since presented analysis does not account for ion Landau damping, it is only accurate for $\omega \gg k_{||}v_{T_i}$ i.e. for ITG mode with $\eta_i \gg 1$, and hence 2/3 is not a precise value for instability threshold. The possibility of instability (15) despite adiabatic electron response highlights the fundamental difference between ITG and electron drift modes, where no instability occur for Boltzmann electrons.

2.2 Physics

Presented model is very useful for the physical understanding of the ITG mode, as discussed in the rest of this section. Specifically, it is instructive to note that in dispersion relations (14, 15) for sound waves,

$$\omega^2 = k^2(\frac{dp}{d\rho}), \tag{16}$$

the $dp/d\rho$ is the compressibility of the medium, and so the instability of ITG mode (15) is due to the negative compressibility $v_{T_i}^2(2/3-\eta_i)$. Note that the ion pressure perturbation $\tilde{p}_i$ is

$$\tilde{p}_i = n_i\tilde{T}_i + \tilde{n}_i T_i = n_i\tilde{T}_i + \frac{|e|\tilde{\Phi}}{T_e}T_i, \tag{17}$$

and so the negative compression is due to the phase difference between the ion temperature perturbation $\tilde{T}_i/T_i$ and density perturbation given by the Boltzmann response $|e|\tilde{\Phi}/T_e$. Such face difference occurs in presence of mean ion temperature gradient, as can be illustrated for the case of large $\nabla\langle T_i\rangle$,

$$\frac{\tilde{T}_i}{T_i} = -\frac{v}{i\omega}\frac{1}{T_i}\frac{\partial\langle T_i\rangle}{\partial r} = -\frac{i\omega_*}{\gamma}\tau_i\frac{e\tilde{\Phi}}{T_e}. \tag{18}$$

To further the understand the physics of instability due to negative compressibility, two other prominent examples are discussed in the interlude below.

2.2.1 Jeans instability

The Jeans instability is an en example of negative compressibility in self gravitating matter. Specifically, from continuity equation

$$\frac{\partial\rho}{\partial t} + \nabla\cdot(\rho\mathbf{v}) = 0, \tag{19}$$

equation of motion

$$\rho\frac{d\mathbf{v}}{dt} = -\nabla p + \rho\nabla\phi \tag{20}$$

and the Poisson equation for the gravitational potential,

$$\nabla^2\phi = 4\pi G\rho \tag{21}$$

follows

$$\frac{\partial^2}{\partial t^2}\tilde{\rho} + \rho\frac{\partial}{\partial t}\nabla\cdot\tilde{\mathbf{v}} = 0,$$

$$\frac{\partial}{\partial t}\nabla\cdot\tilde{\mathbf{v}} = -\frac{\nabla^2\tilde{\rho}}{\rho} - \nabla^2\phi,$$

$$\frac{\partial^2}{\partial t^2}\frac{\tilde{\rho}}{\rho} - \nabla^2 c_s^2\left(\frac{\tilde{\rho}}{\rho}\right) - 4\pi\rho G\frac{\tilde{\rho}}{\rho} = 0,$$

resulting in the dispersion relation

$$\omega^2 = k^2c_s^2 - 4\pi G\rho = k^2c_s^2(1 - \frac{4\pi G\rho_0}{c_s^2k^2}). \tag{22}$$

By the same analogy to the sound waves, $1-4\pi G\rho_0/c_s^2k^2$ is the compressibility that can become negative for sufficiently small k, resulting in the instability.

2.2.2 PSFI

Relative of the ITG, the **P**arallel Shear **F**low $\langle v\rangle_{||}$ **I**nstability occurs due to negative compressibility from the phase shift introduced by $\nabla\langle v_{||}\rangle$. Specifically, for case of flat density and temperature gradients, $\nabla n = \nabla T = 0$, in presence of parallel velocity gradient $v_{||}(r)$, the ion continuity equation

$$\frac{\partial}{\partial t}\frac{e\tilde{\Phi}}{T} + \nabla_{||} v_{||} = 0 \tag{23}$$

in presence of parallel velocity shear

$$\frac{\partial \tilde{v}}{\partial t} = -v_{E_R}\frac{\partial}{\partial r}\langle v_{||}\rangle - c_s^2\nabla_{||}\frac{|e|\tilde{\Phi}}{T} \tag{24}$$

implies

$$\frac{\partial^2}{\partial t^2}\frac{|e|\tilde{\Phi}}{T} + \nabla_{||}(-v_{Er}\frac{\partial\langle v_{||}\rangle}{\partial r} - c_s^2\nabla_{||}\frac{|e|\tilde{\Phi}}{T}) = 0,$$

resulting in dispersion relation

$$\omega^2 = -k_{||}k_\theta\rho_s c_s\frac{\partial\langle v_{||}\rangle}{\partial r} + k_{||}^2c_s^2 = -k_{||}c_s(k_\theta\rho_s\frac{\partial\langle v_{||}\rangle}{\partial r} - k_{||}c_s) \tag{25}$$

Note that the parallel velocity shear $\partial_r\langle v_{||}\rangle$ provides the energy source, and the spectral asymmetry ($k_{||}k_\theta > 0$ needed for instability with $\partial_r\langle v_{||}\rangle < 0$). At critical parallel shear velocity gradient, compressibility becomes negative.

The PSFI can couple to ITG as neutral beam injections puts both heat and the momentum for the parallel shear flow. Due to the coupling, the turbulent viscosity χ_ϕ for the parallel flow is of the order of the ion thermal diffusivity χ_i. The $\chi_\phi \sim \chi_i$ is a robust result owing to the fact that both ITG and PSFI are driven by negative compressibility. The PSFI is most relative to regimes with the flat density profiles as is typical for H-mode, and ind presence of strong eternal torque from unbalanced neutral beam injection.

Coming back to the ITG mode, it is important to reiterate that the energy source is the temperature gradient of ions and the ITG instability is more general than impact of η_i on $v_{T_i}^2(2/3 - \eta_i)$. Specifically, the full dispersion relation (12) in slab geometry suggests that the ITG will still be unstable in the limit of flat density profile

$$1 + \frac{k_{||}^2c_s^2}{\omega^3}\omega_{*T_i} = 0 \Rightarrow \omega = (-1)^{1/3}(k_{||}^2c_s^2\omega_{*T_i})^{1/3}. \tag{26}$$

The flat density regime is particularly relevant to H-mode, and (26) illustrates why "η_i-mode" naming got deprecated in favor of ITG. Furthermore, for toroidal geometry, the stability parameter in addition to η_i also introduces dependence on stabilizing effects from magnetic shear, as well as dependence on R/L_{Ti} and Ln/T_i due to the impact of the curvature $\mathbf{B}\times\nabla B$ drift.

The nature of ITG instability in slab geometry is fundamentally different from the toroidal geometry case. In case of slab η_i mode analyzed above, the negative compressibility transforms the ion acoustic oscillations into unstable compressional waves. In the toroidal model, the curvature drift velocity induces charge separation and the electric field that drives cross-field interchange of plasmas. This provides another mechanism to release the thermal energy stored in ion pressure gradient.
Transition between curvature drift resonance (toroidal ITG branch) and the slab drive was experimentally observed in ITG studies on the Columbia Linear Machine (CLM), where the ITG was studies by starting with the slab mode and gradually increasing the mirror-field.

3 On energy and particle transport

Since ITG instability occurs for the Boltzmann electrons, it can produce heat flux in absence of particle transport. Indeed, since $\tilde{n}/n \sim |e|\tilde{\Phi}/T$ is out of phase with $v_r = \mathbf{v}_\perp \cdot \mathbf{e}_r \propto \mathbf{B} \times \nabla\tilde{\Phi}$, the net particle flux across the magnetic surface $\Gamma = \langle (n+\tilde{n}) v_r \rangle$ is absent. In contrast, the heat flux created by the ITG driven turbulence is typically sufficient to keep the temperature gradients close to marginal threshold, resulting in "stiffness" of the the ion temperature gradient

$$\eta_i - \eta_{i,\mathrm{crit}} \propto P_{OH}^{\alpha}, \text{ where } \alpha \ll 1 \tag{27}$$

Important question related to the ITG-driven turbulent transport is the saturation of ITG by Zonal Flows. Here the feedback loop is established between the turbulence induced Reynolds stress driving the Zonal flow and the resulting Zonal flows suppressing the turbulence by shearing apart the radial turbulent structures.

$$\nabla \cdot \mathbf{v}_{\mathrm{pol}} \to \frac{d}{dt}\nabla_\perp^2 \phi \to \frac{\partial}{\partial r}\langle \tilde{v}_r \nabla^2 \tilde{\phi} \rangle \tag{28}$$

ITG is also an important example of profile corrugations effects, as it results in zonal ion temperature profile corrugation and creations of zonal acoustic flows. Furthermore, ITG leads to generation of zonal acoustic flows, which are an important example of the plasma intrinsic rotation (rotation in absence of external momentum input). The energy for differential rotation in plasma rotation comes from the heat input. The zonal average for parallel flow equation

$$\frac{\partial}{\partial t}\langle v_{||} \rangle + \frac{\partial}{\partial r}\langle \tilde{v}_r \tilde{v}_{||} \rangle + ... = 0 \tag{29}$$

shows the rearrangement of total momentum, with the correlator $\langle \tilde{v}_r \tilde{v}_{||} \rangle$ equal to

$$\langle \tilde{v}_r \tilde{v}_{||} \rangle = \Pi_r \frac{\langle T_i \rangle}{\partial r}, \tag{30}$$

where

$$\Pi_r = \mathbf{Re}\left\{ \sum_n |v_{r,n}|^2 \frac{(-i) v_{T_i}^2 k_{||}}{T_i(\omega_r + 2\gamma i \omega_r - \gamma^2)} \right\}, \tag{31}$$

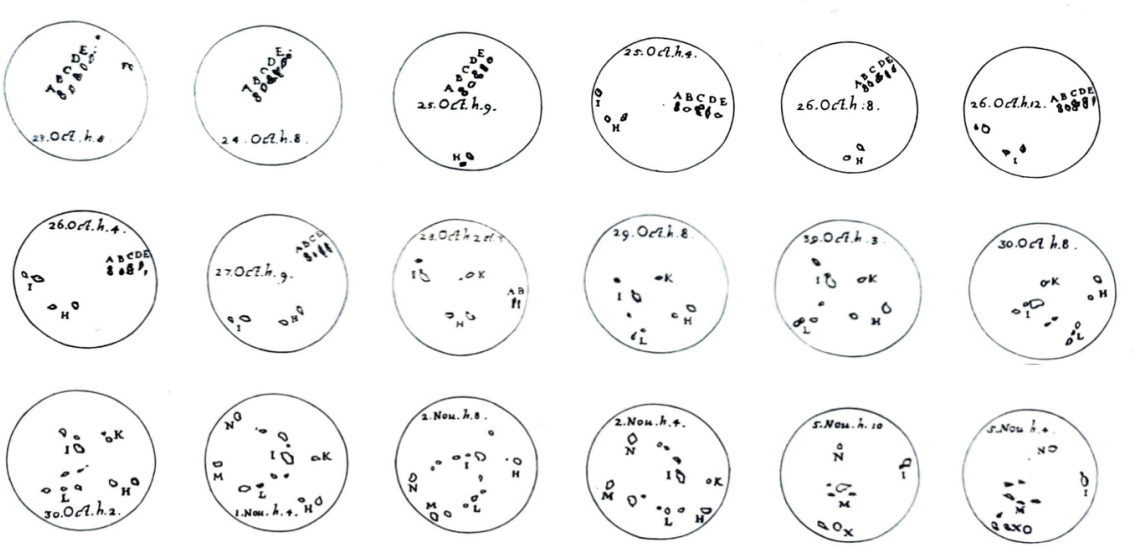

Figure 2: One example of the intrinsic rotation is the differential rotation of the Sun, observed experimentally in 1600s via a time series record of sunspot dynamics. Illustrations by Christopher Scheiner.

implying that the temperature graident $\partial_r \langle T_i \rangle$ can drive the momentum flux in the form to drive a flow. Welcome to intrinsic rotation!

$$\underset{\text{heat goes in}}{Q_{in}} \rightarrow \underset{\text{temperature gradient}}{T_i} \rightarrow \underset{\substack{\text{parallel Reynolds stress} \\ \text{through symmetry braking}}}{\Pi_r} \rightarrow \underset{\text{parallel flow}}{\langle v_{||} \rangle}$$

As was mentioned before, if electrons response is adiabatic there is no particle transport. The net particle transport can result from modifying the Boltzmann response in the basic ITG model by, for example, introducing a phase shift

$$\frac{\tilde{n}_k}{n} = \frac{|e|\tilde{\Phi}_k}{T}\big(1 + i\delta_k\big). \tag{32}$$

This effect of ∇T_i driving the particle flux opens route to the up-gradient transport i.e. the pinch. To understand the driving mechanism for up-gradient particle flux, it is instructive to review the chemotaxis i.e. movement of bacteria in response to the chemical concentration gradient.

3.1 Chemotaxis: the Keller-Segal model

The motion of a microscopic organism can be approximated by random walk. If all bacteria are traveling in the unbiased random walk, the gradients of concentration will diffuse, i.e. the net bacteria flux is always down the concentration slope. However, it is well known in biology that in presence chemical concentration gradient (for example, the "food" for bacteria) can cause the net bacteria flux to be up the bacteria concentration gradient.

Consider a one dimensional model where each bacteria takes steps of length Δ, has the body length $\alpha\Delta$, and has receptors at each side. Assume that the average step frequency $f(c)$depends on the mean concentration c of "food" at the leading edge. Then bacteria located at position x step right with the frequency $f[c(x+0.5\alpha\Delta)]$ and left with $f[c(x-0.5\alpha\Delta)]$. Given the bacteria density $n(x)$, the bacteria flux $\Gamma(x)$ is then

$$\Gamma(x) = \underbrace{\int_{x-\Delta}^{x} f[c(s+0.5\alpha\Delta)]n(s)ds}_{\text{steps to the right}} - \underbrace{\int_{x}^{x+\Delta} f[c(s-0.5\alpha\Delta)]n(s)ds}_{\text{steps to the left}}. \tag{33}$$

Expanding (33) to the first order in Δ gives

$$\Gamma(x) \approx \Delta^2\big(-f[c(x)]n'(x) + (\alpha-1)f'[c(x)]n(x)c'(x)\big), \tag{34}$$

where the first term describes diffusion of bacteria and hence always directed against the density gradient $n'(x)$, and the second term is the chemotaxis response and can be up or down the concentration gradient $c'(x)$ depending on f and α.

The particle flux for the case of non-adiabatic electrons (32) is

$$\Gamma = \langle v_r \frac{\tilde{n}}{n}\rangle = \sum_k i\frac{c_s}{B}k_\theta\tilde{\phi}_k i\delta_k\frac{|e|\tilde{\phi}_k}{T} = -\sum_k c_s(k_\theta\rho_s)\delta_k\left|\frac{e\tilde{\phi}_k}{T}\right|^2, \tag{35}$$

where $\delta_k = \delta n/\delta(|e|\phi/T)$ is set by the non-adiabatic electron response and is the phase shift between the density and potential. Negative $\delta_k < 0$ results in the outward flux, while $\delta_k < 0$ results in inward flux. This can be related to the Keller-Segal model, as δ_k is effectively encoding the "food" while the fluctuation level $|e\tilde{\phi}_k|/T$ accounts for the energy for the steps. The response of δ_k to the density gradient $\delta\delta_k/\delta\nabla n$ has to be positive to comply with entropy production i.e. no negative particle diffusion should be possible. From second law of thermodynamics

$$\frac{\partial S}{\partial t} \sim -\Gamma\nabla n = D\nabla^2 n - \sigma n\nabla n\nabla c > 0 \tag{36}$$

follows that the concentration gradients allows for some entropy destruction by the up-gradient flux. So, since up-gradient non-adiabatic particle flux driven by electrons can not be produced by the density gradient, it has to be driven by the electron temperature. The pinch is ultimately due to the electron temperature gradient, with ∇T_e

corresponding to gradient in concentration of "food" supply ∇c in Keller-Segal model. Therefore, $\delta\delta_k/\delta\nabla T_e < 0$ for the pinch and hence the temperature gradient and the density gradient from the non-adiabatic electron response have to have opposite phases, arriving to the concept of "Ion Mixing Mode" i.e. the ITG mode with collisional non-adiabatic electron response that involves ∇T_e. The electron temperature gradient shifts the sign of δ_k to make the convection velocity negative $V < 0$. Part of the physics of the Ion Mixing Mode is shown on the scheme below:

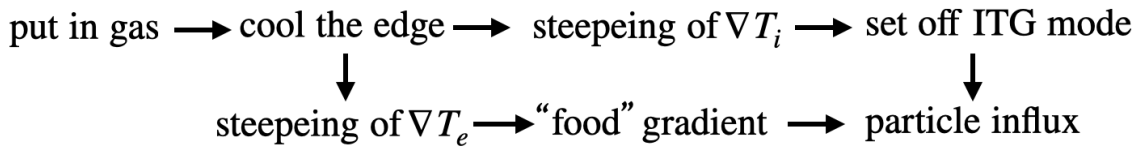

One needs to ensure the positive net entropy production,

$$\frac{\partial}{\partial t}\frac{S}{nT} = -\frac{\nabla\langle n\rangle}{n}\Gamma_n - \frac{\nabla T_i}{T}Q_{\mathrm{T_i}}, \tag{37}$$

equal to

$$\frac{\partial}{\partial t}\frac{S}{nT} = \chi_i\Big(\frac{\nabla T_i}{T}\Big)^2 + O\Big(\frac{\omega}{\chi_{||}k_{||}^2}\Big) - \frac{\nabla\langle n\rangle}{n}\Gamma_n. \tag{38}$$

The second term in (38) is the growth rate correction and the last term is the positive but small. In conclusion, more entropy is produced by relaxing the ion temperature gradient than lost due to density peaking by the pinch. i.e. the relaxation of ∇T_i dominates the entropy production. Summarizing the analogy with the Keller-Segal model,

pinch	Keller-Segal
density	bacterial density
electron temperature gradient ∇T_e	"food" supply gradient∇c
ion temperature gradient ∇T_i	bacterial energy
phases	food sensors